5. J. J. Pluth and J. V. Smith, *Am. Mineral.* **75**, 501 (1990).
6. M. D. Shannon *et al.*, *Nature* **353**, 417 (1991).
7. S. I. Zones, M. M. Olmstead, D. S. Santilli, *J. Am. Chem. Soc.* **114**, 4195 (1992).
8. S. I. Zones *et al.*, U.S. Patent 4 910 006 (1990).
9. S. I. Zones, U.S. Patent 4 963 337 (1990).
10. J. M. Newsam, M. M. J. Treacy, W. T. Koetsier, C. B. de Gruyter, *Proc. R. Soc. London Ser. A* **420**, 375 (1988).
11. M. D. Shannon, in *Proceedings of the 9th International Zeolites Conference*, R. von Ballmoos, J. B. Higgins, M. M. Treacy, Eds. (Butterworth-Heinemann, Stoneham, MA, 1993), vol. 1, pp. 389–398.
12. M. Pan and P. A. Crozier, *Ultramicroscopy* **48**, 322 (1993).
13. ———, *ibid.*, in press.
14. M. Pan *et al.*, in preparation.
15. C. Baerlocher, A. Hepp, W. M. Meier, *DLS-76* (Institut fur Kristallographie, ETH, Zürich, 1976). The weighted agreement values for polymorph A were $R = 0.0013$, $\sigma = 0.007$ and for polymorph B were $R = 0.001$, $\sigma = 0.005$. The unit cell dimensions were held constant during the optimization by using the values obtained from the indexing of the synchrotron XRD pattern of SSZ-33. $\langle T\text{–}O \rangle = 1.60$ Å [assuming Si:B = 15, Si–O = 1.605 Å (*10*), and B–O = 1.48 Å].
16. The distance least squares refinement and the simulation of the XRD patterns of polymorph A and polymorph B were carried out with the program CERIUS 3.1 from Molecular Simulations.
17. M. M. J. Treacy, M. W. Deem, J. M. Newsam, *Proc. R. Soc. London Ser. A* **433**, 499 (1991). The simulations were carried out with the atom positions obtained from the distance least squares optimization of polymorph A. Silicon was used in all T atom positions.
18. R. F. Lobo *et al.*, in preparation.
19. S. I. Zones and D. S. Santilli, in *Proceedings of the 9th International Zeolites Conference*, R. von Ballmoos, J. B. Higgins, M. M. Treacy, Eds. (Butterworth-Heinemann, Stoneham, MA, 1993), vol. 1, pp. 171–179.
20. We are grateful to Chevron Research and Technology Company for financial support. We thank W. P. Schaefer and R. E. Marsh for comments on the manuscript. We acknowledge D. E. Cox for assistance in collecting the synchrotron data. The XRD data were collected at X7A beam line, National Synchrotron Light Source, Brookhaven National Laboratory, which is supported by the Department of Energy, Division of Material Sciences and Division of Chemical Sciences. We also acknowledge the assistance of G. Zhang and G. Mondo, from Chevron Research and Technology Company, in collecting the synchrotron data. M.P. and P.A.C. were supported by the HREM Industrial Associates Program at Arizona State University. HREM work was done at the Center for HREM at Arizona State University supported by NSF grant DMR9115680.

7 July 1993; accepted 7 October 1993

Engineered Biosynthesis of Novel Polyketides

Robert McDaniel, Susanne Ebert-Khosla, David A. Hopwood, Chaitan Khosla*

Polyketide synthases (PKSs) are multifunctional enzymes that catalyze the biosynthesis of a huge variety of carbon chains differing in their length and patterns of functionality and cyclization. Many polyketides are valuable therapeutic agents. A *Streptomyces* host-vector system has been developed for efficient construction and expression of recombinant PKSs. Using this expression system, several novel compounds have been synthesized in vivo in significant quantities. Characterization of these metabolites has provided new insights into key features of actinomycete aromatic PKS specificity. Thus, carbon chain length is dictated, at least in part, by a protein that appears to be distinctive to this family of PKSs, whereas the acyl carrier proteins of different PKSs can be interchanged without affecting product structure. A given ketoreductase can recognize and reduce polyketide chains of different length; this ketoreduction always occurs at the C-9 position. The regiospecificity of the first cyclization of the nascent polyketide chain is either determined by the ketoreductase, or the chain-extending enzymes themselves. However, the regiospecificity of the second cyclization is determined by a distinct cyclase, which can discriminate between substrates of different chain lengths.

Polyketides occur in most groups of organisms and are especially abundant in a class of mycelial bacteria, the actinomycetes. They are an extremely rich source of bioactive molecules, including antibiotics (such as tetracyclines and erythromycin), anticancer agents (daunomycin), immunosuppressants (FK506 and rapamycin), and veterinary products (monensin and avermectin). Like the related fatty-acid synthases (FASs), the polyketide synthases (PKSs) are multifunctional enzymes that catalyze repeated decarboxylative condensations between coenzyme A (CoA) thioesters (usually acetyl, propionyl, malonyl, or methylmalonyl). After each condensation, FASs typically catalyze a complete reductive cycle comprising a ketoreduction, dehydration, and enoylreduction on the β-keto group of the growing carbon chain, whereas PKSs omit this cycle or curtail it after some or even all condensation steps. After the carbon chain has grown to a length characteristic of each specific product, it is released from the synthase by thiolysis or acyltransfer (*1*). It is the controlled variation in chain length, choice of chain-building units, and the reductive cycle, genetically programmed into each PKS, that leads to the huge variation among naturally occurring polyketides (*2*).

Although the rules of this programming have hitherto been obscure, current genetics-led research is beginning to clarify them. Cloning and sequencing of PKS genes has suggested two entirely different programming strategies. One is represented by the PKSs for macrolides such as erythromycin, which consist of several large multifunctional proteins carrying, between them, a set of separate active sites for every individual step of carbon-chain assembly and modification (*3*). There is thus a one-to-one correlation between the number and clustering of active sites in the primary sequence of the PKS and the structural features of the polyketide backbone. The second class of PKSs, represented by the synthases for aromatic compounds, has a single set of iteratively used active sites (*4–6*). It follows that the programming mechanism for this class of PKS is not apparent from the number and arrangement of active sites.

We report the development of a *Streptomyces* host-vector system that allows the facile construction of minimal sets of genes for natural or hybrid combinations of PKS components (or mutants thereof) and the expression of the gene sets to produce novel polyketide products. The advantages of the system are that the genes are expressed in a quasi-natural manner to produce significant quantities of product at an appropriate stage of the growth cycle, and that the products themselves undergo a minimum of post-PKS reactions. Thus, determination of product structure gives direct insights into aspects of PKS programming. The results reported here include the discovery that a specific component of the PKS is responsible, at least in part, for determining carbon chain length, that either the ketoreductase or the chain-extending enzymes play a key role in dictating the regiospecificity of the first cyclization of the nascent carbon chain, and that further cyclization is determined by the specificity of a cyclase. Five new compounds generated by this system are reported here and elsewhere (*7*). The system holds great promise for the generation of a wide range of potentially useful metabolites.

Streptomyces coelicolor A3(2), a model actinomycete with well-developed genetics (*8*), produces the blue-pigmented polyketide, actinorhodin (*1*) (Fig. 1). The biosynthetic pathway has been partially elucidated (*9–11*), and the *act* gene cluster has

R. McDaniel, S. Ebert-Khosla, C. Khosla, Department of Chemical Engineering, Stanford University, Stanford, CA 94305–5025.
D. A. Hopwood, Department of Genetics, John Innes Institute, John Innes Centre, Norwich NR4 7UH, United Kingdom.

*To whom correspondence should be addressed.

been cloned (*12*) and completely sequenced (*5, 13, 14*). It encodes the PKS (the collection of active sites that catalyze the biosynthesis of the appropriately reduced octaketide and also dictate regiochemistry of the first cyclization), a cyclase, and a series of tailoring enzymes involved in subsequent modification reactions leading to actinorhodin as well as proteins involved in export of the antibiotic and at least one protein that specifically activates transcription of the gene cluster (Fig. 2A). Other genes required for global regulation of antibiotic biosynthesis are located outside the *act* cluster (*15*); this is also believed to be true for the genes for the supply of starter (acetyl CoA) and extender (malonyl CoA) units for polyketide biosynthesis.

The host strain CH999 of *S. coelicolor* (Fig. 2B) was constructed by deleting, through a homologous recombination, the entire *act* cluster from the chromosome of a strain lacking endogenous plasmids and carrying a stable mutation that blocks biosynthesis of another pigmented *S. coelicolor* antibiotic, undecylprodigiosin. pRM5 (Fig. 2C) is the shuttle plasmid used for expressing PKSs in CH999. It includes a *ColE*I replicon to allow genetic engineering in *Escherichia coli*, an appropriately truncated SCP2* (low copy number) *Streptomyces* replicon, and the *act*II-ORF4 activator gene from the *act* cluster, which induces transcription from *act* promoters during the transition from growth phase to stationary phase (*16*). pRM5 carries the divergent *actI*/*act*III promoter pair, together with convenient cloning sites to facilitate the insertion of a variety of engineered PKS genes downstream of both promoters (*17*). This means that recombinant PKSs are expressed approximately at the transition from exponential to stationary phase of growth and in good yield.

In each *Streptomyces* aromatic PKS so far studied, carbon-chain assembly requires the products of three open reading frames (ORFs) (*4–6*): ORF1 encodes a ketosynthase (KS) and a putative acyltransferase (AT) active site; ORF2 encodes a protein similar to the ORF1 product but lacking the KS and AT motifs and of unknown function before the experiments described here; and ORF3 encodes a discrete acyl carrier protein (ACP). To facilitate replacements of *act* ORFs 1 to 3, they were cloned in pRM5 as individual cassettes with flanking restriction sites and their own ribosome binding sites (RBSs) with the polymerase chain reaction (PCR) (*18*). To construct the recombinant PKSs described below (Table 1), other naturally occurring ORF1 and ORF2 alleles were also cloned as exchangeable cassettes with the same flanking sequences.

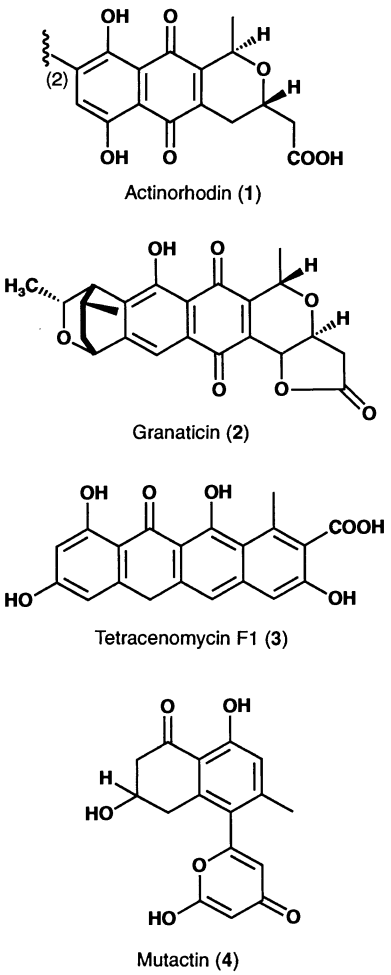

Fig. 1. Structures of four previously characterized polyketides. For details see text.

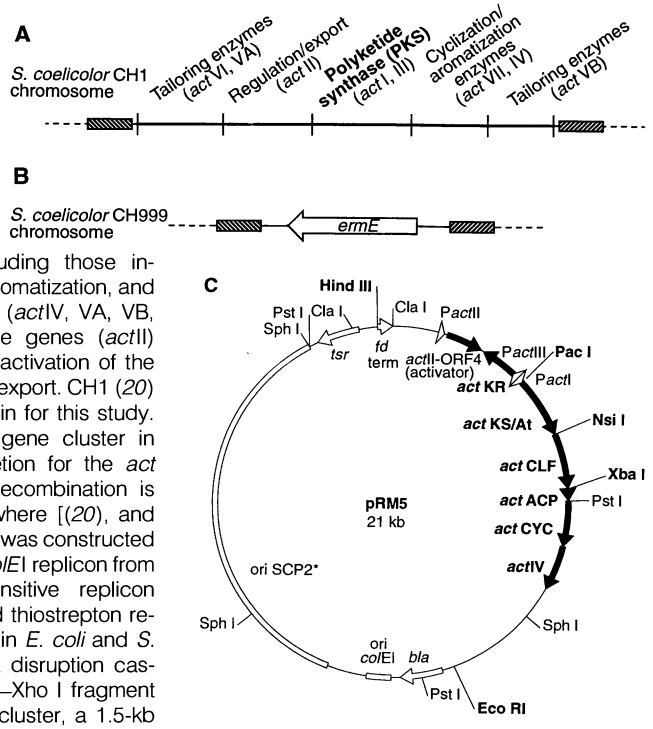

Fig. 2. Construction of a *S. coelicolor* host-vector system for the expression of recombinant PKSs. (**A**) The *act* gene cluster, encoding biosynthesis and export of the polyketide antibiotic actinorhodin, is made up of the PKS genes (*act*I and III), flanked by several post-PKS biosynthetic genes including those involved in cyclization (*act*VII), aromatization, and subsequent chemical tailoring (*act*IV, VA, VB, and VI). Also present are the genes (*act*II) responsible for transcriptional activation of the *act* genes and for actinorhodin export. CH1 (*20*) was chosen as the parent strain for this study. (**B**) Replacement of the *act* gene cluster in CH999. The strategy for deletion for the *act* cluster through homologous recombination is similar to that described elsewhere [(*20*), and references therein]. pLRermEts was constructed with the following features: a *ColE*I replicon from pBR322, the temperature-sensitive replicon from pSG5 (*29*), ampicillin and thiostrepton resistance markers for selection in *E. coli* and *S. coelicolor*, respectively, and a disruption cassette including a 2-kb Bam HI–Xho I fragment from the "left" end of the *act* cluster, a 1.5-kb *ermE* fragment conferring lincomycin resistance (*20*), and a 1.9-kb Sph I–Pst I fragment from the "right" end of the *act* cluster. The left fragment extended from Bam HI site 1 (*12*) rightward to a Xho I site. The "right" fragment extended from Pst I site 20 leftward to Sph I site 19.2 (*5*). The "left" and "right" fragments (shown as hatched DNA) were cloned in the same relative orientation as in the *act* cluster. CH1 was transformed with pLRermEts. The plasmid was subsequently cured from candidate transformants by nonselective growth at 39°C. Several colonies that were lincomycin resistant, thiostrepton sensitive, and unable to produce actinorhodin were isolated and checked through DNA blotting. One of them was designated CH999. Genomic DNA fragments are not drawn to scale. (**C**) pRM1, the progenitor of pRM5, was constructed by ligating the 10.5-kb Sph I–Hind III fragment from pIJ903 (containing a portion of the fertility locus and the origin of replication of SCP2* as well as the *ColE*I origin of replication and the β-lactamase gene from pBR327) (*30*) with a 1.5-kb Hind III–Sph I *tsr* gene cassette. pRM5 was constructed by inserting the following two fragments between the unique Hind III and Eco RI sites of pRM1: a 0.3-kb Hind III–Hpa I (blunt) fragment carrying a transcription terminator from phage fd (*20*), and a 10-kb fragment from the *act* cluster extending from the Nco I site (1 kb upstream of the *act*II-ORF4 activator gene) (*13*) to the Pst I site (site 20) downstream of the *act*I-VII-IV genes (*5*). To facilitate the expression of any desired recombinant PKS under the control of the *act*I promoter (which is activated by the *act*II-ORF4 gene product), restriction sites for Pac I, Nsi I, Xba I, and Pst I were engineered into the *act* DNA in intercistronic positions as described in the text and in (*18*). In pRM5, as well as in all other PKS expression plasmids described here, ORF 1, 2, and 3 alleles were cloned between these sites as cassettes engineered with their own RBSs [for details, see (*18*)].

The *act* KS/AT, the ORF2 gene product, and ACP constitute a "minimal" PKS; studies on PKS mutants showed that mutations in any one of the genes encoding these functions abolish PKS activity (*5, 19, 20*). In addition to these three genes, pRM5 carries the *act*III ketoreductase (KR) gene, the cyclase gene (*act*VII), and a putative dehydratase gene (*act*IV) (*13, 21*). The expectation was that co-expression of these six genes would lead to the biosynthesis of the nascent PKS product and its conversion into a stable but minimally modified anthraquinone-like structure (*11*), as opposed to a tetralone-pyrone–like structure, mutactin (**4**) (Fig. 1), which is produced as a result of spontaneous cyclizations in an *act*VII mutant (*10*).

Transformation of CH999 by pRM5 caused it to produce a large amount of yellowish-brown material. The two most abundant products were characterized as aloesaponarin II (**5**) (*11*) and its carboxylated analog, 3,8-dihydroxy-1-methylanthraquinone-2-carboxylic acid (**6**) (*22*) (Fig. 3). It is presumed that **5** is derived from **6** by non-enzymatic decarboxylation (*11*). Compounds **5** and **6** were present in approximately a 1:5 molar ratio. Approximately 100 mg of the mixture could be easily purified from 1 liter of culture. Evidently, the CH999/pRM5 host-vector system was functioning as expected to produce significant amounts of a stable, only minimally modified, polyketide metabolite. The production of **5** and **6** is consistent with the proposed pathway of actinorhodin biosynthesis (*11*). Both metabolites, like the actinorhodin backbone, are derived from a 16-carbon polyketide with a single ketoreduction at C-9. Indeed, the set of genes on pRM5 includes just those biosynthetic genes whose products would act on the primary polyketide in an *act*VI mutant, previously shown to produce **5** (*11*).

When CH999 was transformed with pSEK4, identical to pRM5 except for inactivation of the *act* KR gene by replacement of an internal 140-bp Sph I–Sal I fragment by the Sph I–Sal I fragment from pUC19, the resulting strain produced abundant quantities of an aromatic polyketide. Although the exact structure of this product has not yet been elucidated, it is significantly different from that of the anticipated product, desoxyerythrolaccin (*11*). Preliminary studies suggest that the polyketide backbone of this product is derived from eight acetates and is not reduced.

In an attempt to generate novel polyketides differing in a range of properties, as well as to elucidate aspects of the programming of aromatic PKSs, a systematic series of minimal PKS gene clusters was constructed and analyzed. As shown in Fig. 4, the PKSs responsible for synthesizing the carbon-chain backbones of actinorhodin (**1**), granaticin (**2**), and tetracenomycin (**3**) contain homologous putative KS/AT, ORF2 product, and ACP subunits (*4, 5*). The *act* and *gra* PKSs also have KRs lacking in the *tcm* PKS. Corresponding proteins

Table 1. Polyketides produced by homologous and heterologous combinations of PKS proteins. The *act* ORFs 1, 2, and 3 of pRM5 were replaced with corresponding homologs from *gra* and *tcm*. The resulting plasmids were introduced into *S. coelicolor* CH999 by transformation and the major products identified. NP signifies no detectable polyketide was produced.

Plasmid	ORF1 (KS/AT)	ORF2 (CLF)	ORF3 (ACP)	Major product	Backbone carbon length
pRM5	*act*	*act*	*act*	**5,6**	16
pRM7	*gra*	*act*	*act*	**5,6**	16
pRM12	*act*	*gra*	*act*	**5,6**	16
pRM22	*act*	*act*	*gra*	**5,6**	16
pRM10	*tcm*	*act*	*act*	**5,6**	16
pRM15	*act*	*tcm*	*act*	NP	
pRM20	*tcm*	*tcm*	*act*	**7**	20
pRM25	*act*	*act*	*tcm*	**5,6**	16
pRM35	*tcm*	*act*	*tcm*	**5,6**	16
pRM36	*act*	*tcm*	*tcm*	NP	
pRM37	*tcm*	*tcm*	*tcm*	**7**	20

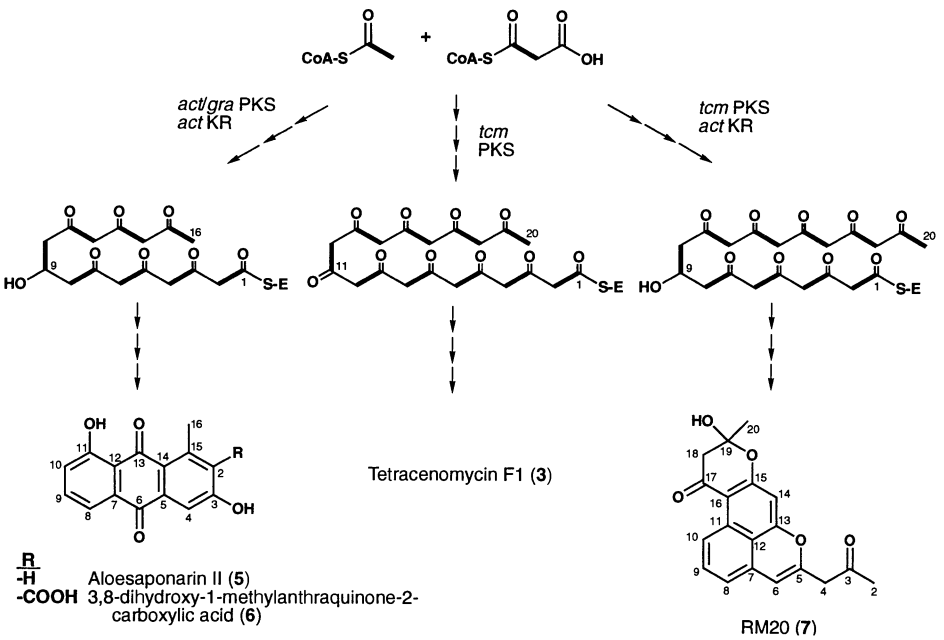

Fig. 3. Structures and deduced backbones of polyketides synthesized by recombinant PKSs. Bold bonds illustrate the pattern of acetate incorporation in backbone biosynthesis. Structural elucidation was performed by nuclear magnetic resonance (NMR) spectroscopy. The ^{1}H and ^{13}C spectra of **5** and **6** were identical to published data (*11, 22*). The ^{1}H and ^{13}C spectral assignments for **7** are listed below. Nuclear Overhauser effect (NOE) interactions for each hydrogen were measured and are consistent with the proposed structure of **7**. Furthermore, the structure and chemical shifts of **7** are similar to those of RM18, which has been characterized more extensively (*7*). The materials and methods for feeding, purification, and characterization of these compounds are analogous to those described elsewhere (*7*). Coupling constants for the ^{13}C spectrum refer to carbon-carbon couplings determined through [1,2-$^{13}C_2$] acetate incorporation. **7**: 400-MHz ^{1}H NMR (DMSO-d_6) δ(ppm) 9.00 (d, J = 8.8 Hz, 1H, C-10), 7.51 (dd, J = 7.0,8.8 Hz, 1H, C-9), 7.14 (s, 1OH,C-19), 6.94 (d, J = 7.0 Hz, 1H, C-8), 6.37 (s, 1H, C-14), 6.31 (s, 1H, C-6), 3.67 (s, 2H, C-4), 3.05 (d, J = 16.0 Hz, 1H, C-18), 2.67 (d, J = 16.0 Hz, 1H, C-18), 2.21 (s, 3H, C-2), and 1.60 (s, 3H, C-20); 100-MHz ^{13}C NMR (DMSO-d_6) δ(ppm) 203.7 (J = 36.8 Hz, C-3), 190.7 (J = 39.9 Hz, C-17), 162.9 (J = 63.8 Hz, C-15), 158.4 (J = 75.0 Hz, C-13), 149.6 (J = 77.2 Hz, C-5), 132.6 (J = 56.1 Hz, C-11), 131.8 (J = 57.5 Hz, C-9), 129.0 (J = 61.5 Hz, C-7), 121.7 (J = 57.9 Hz, C-10), 117.4 (J = 55.7 Hz, C-12), 116.1 (J = 61.4 Hz, C-8), 107.2 (J = 76.7 Hz, C-6), 106.4 (J = 63.6 Hz, C-16), 101.6 (J = 46.0 Hz, C-19), 99.0 (J = 74.7 Hz, C-14), 49.4 (J = 39.7 Hz, C-18), 46.9 (J = 37.1 Hz, C-4), and 29.6 (enriched but not coupled, C-2), 27.3 (J = 45.8 Hz, C-20). Field desorption mass spectroscopy gave a mass-to-charge ratio of 325.

from each cluster show a high degree of sequence identity (caption to Fig. 4). The *act* and *gra* PKSs synthesize identical 16-carbon backbones derived from eight acetate residues with a ketoreduction at C-9 (Fig. 3). In contrast, the *tcm* polyketide backbone differs in overall carbon chain length (20 instead of 16 carbons), lack of any ketoreduction, and regiospecificity of the first cyclization, which occurs between carbons 9 and 14, instead of carbons 7 and 12 for *act* and *gra* (Fig. 3).

Analysis of the products of the recombinant PKSs containing various permutations of the KS/AT, ORF2 product, and ACP subunits of the PKSs (all constructs also containing the *act* KR, cyclase, and dehydratase genes) indicated that the synthases could be grouped into three categories (Table 1): those that did not produce any polyketide; those that produced compound **6** (in addition to its analog **5**); and those that produced a novel polyketide **7** (designated RM20) (Fig. 3). Sodium [1,2-$^{13}C_2$] acetate feeding experiments indicate that the polyketide backbone precursor of **7** is derived from 10 acetate residues with a single ketoreduction at the C-9 position.

In order to investigate the influence of the *act* KR on the reduction and cyclization patterns of a heterologous polyketide chain, we also constructed pSEK15 carrying *tcm* ORFs 1 to 3 but lacking the *act* KR. (The deletion in the *act* KR gene in this construct was identical to that in pSEK4 described above.) Analysis of CH999/pSEK15 led to the purification of yet another distinct polyketide product, whose structure is currently being elucidated (*23*). Nuclear magnetic resonance spectroscopy nevertheless was consistent with a completely unreduced decaketide backbone.

All of the *act/gra* hybrids produced compound **6**, consistent with the identical structures of the presumed actinorhodin and granaticin primary polyketides. In each case where a product could be isolated from a *tcm/act* hybrid, the chain length of the polyketide was identical to that of the natural product corresponding to the source of ORF2. This finding suggests that the ORF2 product controls carbon-chain length. However, because we could not generate a functional ORF1/ORF2 hybrid in which the KS/AT is derived from the shorter chain PKS, it is also possible that both the KS/AT and the ORF2 product are capable of exercising some chain-length control. By comparing the structures of the three reduced polyketides described here (that is, **5**, **6**, and **7**), one can also conclude the following: (i) the KR is both necessary and sufficient for ketoreduction to occur; (ii) this reduction always occurs at the C-9 position of the final polyketide backbone (counting from the carboxyl end of the chain) (*24*); and (iii) the regiospecificity of ketoreduction is constant relative to that of the first cyclization, suggesting that both these events are controlled by either the ketoreductase or the chain-extending enzymes.

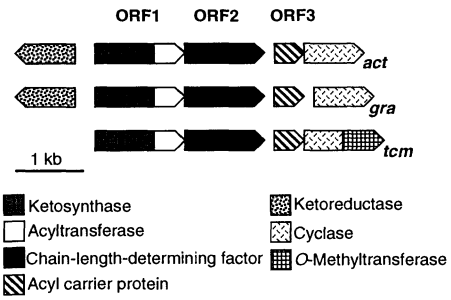

Fig. 4. Gene clusters for *act*, *gra*, and *tcm* PKSs and cyclases. The percentage identities between corresponding PKS proteins in the three clusters are as follows: KS/AT: *act/gra* 76, *act/tcm* 64, *gra/tcm* 70; CLF: *act/gra* 60, *act/tcm* 58, *gra/tcm* 54; ACP: *act/gra* 60, *act/tcm* 43, and *gra/tcm* 44. [Note that the carboxyl-terminal halves of the *act* and *gra* cyclases have previously been postulated to catalyze dehydration reactions in carbon chain modification (*21*).]

A striking feature of RM20 is the pattern of cyclizations following the first cyclization. Isolation of mutactin (**4**) from an *act*VII mutant suggested that the *act*VII product and by analogy its *tcm* homolog catalyze the cyclization of the second ring in the biosynthesis of actinorhodin (**1**) and tetracenomycin (**3**), respectively (*21*, *25*). The cyclization pattern of RM20 is different from that of **6** and tetracenomycin F1, despite the presence of the *act*VII gene on pRM20. It therefore appears that the *act* cyclase cannot cyclize longer polyketide chains. This inactivity could be due to its inability either to recognize longer chain substrates or to associate productively with PKS components that synthesize longer carbon chains.

No polyketide could be detected in CH999/pRM15 or CH999/pRM36 (Table 1). Thus, only some ORF1-ORF2 combinations are functional. Because each subunit was functional in at least one recombinant synthase, protein expression and folding problems are unlikely to be the cause. Instead, imperfect or inhibitory association between the different subunits of these enzyme complexes, or biosynthesis of (aborted) short chain products that are chemically unstable, are plausible explanations.

The above results are consistent with those of similar experiments in which a polyketide synthase of unproven function was used (*7*).

Until now, the function of the ORF2 product in aromatic PKSs has been unknown. It has been suggested that the ORF1 and ORF2 products function as a heterodimer (*4*). The results reported above suggest that the ORF2 product plays the role of a chain-length-determining factor (CLF). The simplest model is one in which the CLF is a thioesterase. Such a mechanism for chain-length control occurs in plant FASs (*26*). Alternatively, the CLF (perhaps in conjunction with the KS/AT) could provide a water-excluding binding pocket with appropriate molecular dimensions and noncovalent interactions for the nascent polyketide chain. Further in vivo and in vitro studies of aromatic CLFs are necessary in order to conclusively explain the role of this protein. The above expression system can serve as a source of functional mutant PKSs to aid such in vitro mechanistic studies (*27*).

In the course of the studies described above and elsewhere (*7*), five novel molecules have already been produced. The expression system provides a practical method for designing and synthesizing other polyketides by allowing the genetic engineer to build a PKS with only the desirable components. In view of the minimal number of modification reactions that such compounds undergo, they would be particularly attractive targets for subsequent synthetic derivatization. As shown for the frenolicin PKS, the system can also be used to functionally express PKSs of uncertain (and possibly even unknown) specificities, that can be easily cloned by homology (*6*, *7*, *28*). Given the size of the PKS gene family in nature and the availability of suitable gene probes for different subgroups of PKSs in diverse organisms including bacteria, fungi, plants, and animals, this approach could be an effective method for the biosynthesis of large numbers of novel structures.

Our results demonstrate that at least three factors that control elements of aromatic polyketide structural diversity (that is, chain length, ketoreduction, and the regiospecificity of cyclizations) can be effectively exploited to produce novel polyketides. The eventual impact of the strategy described here will be critically determined by the following four factors: (i) its applicability to the biosynthesis of other classes of polyketides, including the modular PKSs for compounds such as macrolides, polyenes, and polyethers; (ii) the extent to which the various classes of PKSs will tolerate changes introduced by targeted mutagenesis or by replacement of domains or subunits; (iii) the ease of isolating naturally occurring homologs of domains or subunits that control variability in polyketide structure; and (iv) the substrate plasticity of naturally occurring post-PKS tailoring enzymes that may be co-expressed in strains producing alterna-

tive polyketides to convert the unmodified primary PKS products into interesting metabolites.

REFERENCES AND NOTES

1. S. J. Wakil, *Biochemistry* **28**, 4523 (1989); D. O'Hagan, *The Polyketide Metabolites* (Horwood, Chichester, 1991).
2. D. A. Hopwood and D. H. Sherman, *Annu. Rev. Genet.* **24**, 37 (1990); J. Robinson, *Philos. Trans. R. Soc. London Ser. B* **332**, 107 (1991); D. A. Hopwood and C. Khosla, in *Secondary Metabolites, Their Function and Evolution*, vol. 171 of the *Ciba Foundation Symposium Series* (Wiley, New York, 1992), pp. 88–112; C. R. Hutchinson *et al.*, *Actinomycetology* **6**, 49 (1992); L. Katz and S. Donadio, *Annu. Rev. Microbiol.* **47**, 875 (1993).
3. J. Cortes, S. F. Haydock, G. A. Roberts, D. J. Bevitt, P. F. Leadlay, *Nature* **348**, 176 (1990); S. Donadio, M. J. Staver, J. B. McAlpine, S. J. Swanson, L. Katz, *Science* **252**, 675 (1991); D. J. MacNeil *et al.*, *Gene* **115**, 119 (1992).
4. M. J. Bibb, S. Biro, H. Motamedi, J. F. Collins, C. R. Hutchinson, *EMBO J.* **8**, 2727 (1989); D. H. Sherman *et al.*, *ibid.*, p. 2717.
5. M. A. Fernandez-Moreno, E. Martinez, L. Boto, D. A. Hopwood, F. Malpartida, *J. Biol. Chem.* **267**, 19278 (1992).
6. M. J. Bibb, D. H. Sherman, S. Omura, D. A. Hopwood, unpublished results.
7. R. McDaniel, S. Ebert-Khosla, D. A. Hopwood, C. Khosla, *J. Am. Chem. Soc.*, in press.
8. D. A. Hopwood *et al.*, Eds., *Genetic Manipulation of* Streptomyces: *A Laboratory Manual* (John Innes Foundation, Norwich, United Kingdom, 1985); T. Kieser and D. A. Hopwood, *Methods Enzymol.* **204**, 430 (1991).
9. S. P. Cole, B. A. M. Rudd, D. A. Hopwood, C. J. Chang, H. G. Floss, *J. Antibiot.* **40**, 340 (1987).
10. H. L. Zhang *et al.*, *J. Org. Chem.* **55**, 1682 (1990).
11. P. L. Bartel *et al.*, *J. Bacteriol.* **172**, 4816 (1990).
12. F. Malpartida and D. A. Hopwood, *Nature* **309**, 462 (1984); F. Malpartida and D. A. Hopwood, *Mol. Gen. Genet.* **205**, 66 (1986).
13. S. E. Hallam, F. Malpartida, D. A. Hopwood, *Gene* **74**, 305 (1988); M. A. Fernandez-Moreno, J. L. Caballero, D. A. Hopwood, F. Malpartida, *Cell* **66**, 769 (1991); J. L. Caballero, E. Martinez, F. Malpartida, D. A. Hopwood, *Mol. Gen. Genet.* **230**, 401 (1991).
14. F. Malpartida, personal communication.
15. K. F. Chater, in *Secondary Metabolites, Their Function and Evolution*, vol. 171 of the *Ciba Foundation Symposium Series* (Wiley, New York, 1992), pp. 144–162.
16. H. C. Gramajo, E. Takano, M. J. Bibb, *Mol. Microbiol.* **7**, 837 (1993).
17. The expression vector pRM5 lacks the *par* locus of SCP2*; as a result the plasmid is slightly unstable (~2% loss, as measured by one round of plating in the absence of thiostrepton). This feature was deliberately introduced in order to allow for rapid confirmation that a phenotype of interest was specified by the plasmids.
18. In most naturally occurring aromatic polyketide synthase gene clusters in actinomycetes [see, for example, (*4*–*6*)], ORF1 and ORF2 are translationally coupled, with a (weak) RBS for ORF2 within the ORF1 coding sequence. In order to facilitate construction of recombinant PKSs, the ORF1 and ORF2 alleles used here were cloned as independent (uncoupled) cassettes, each with a discrete RBS. For *act* ORF1, the following sequence was engineered into pRM5: **CCACCGGACGAACGCATCG**ATTAATT AAggaggACCATCATG, where the boldfaced sequence corresponds to upstream DNA from the *act*I region, TTAATTAA is the Pac I recognition site, ATG is the start codon of *act* ORF1, and the lower case letters denote the RBS. The following sequence was engineered between *act* ORF1 and ORF2: NTGAATGCATggaggAGCCATCATG, where TGA and ATG are the stop and start codons of ORF1 and ORF2, respectively, ATGCAT is the Nsi I recognition site, and the replacement of N (A in *act* DNA, A or G in alleles from other PKSs) with a C results in translational decoupling. The following sequence was engineered downstream of *act*I ORF2: TAATCTAGA, where TAA is the stop codon, and TCTAGA is the Xba I recognition site. This allowed fusion of *act* ORF1 + ORF2 (engineered as above) to an Xba I site that had been engineered upstream of *act* ORF3 (*20*). As a control, pRM2 was constructed, identical to pRM5, but lacking any of the engineered sequences, so that ORF1 and ORF2 are translationally coupled. Comparison of the product profiles of CH999/pRM2 and CH999/pRM5 revealed that the decoupling strategy described here had no detectable influence on product distribution or levels.
19. D. H. Sherman, E. S. Kim, M. J. Bibb, D. A. Hopwood, *J. Bacteriol.* **174**, 6184 (1992).
20. C. Khosla, S. Ebert-Khosla, D. A. Hopwood, *Mol. Microbiol.* **6**, 3237 (1992).
21. D. H. Sherman *et al.*, *Tetrahedron* **47**, 6029 (1991).
22. D. W. Cameron, D. J. Deutscher, G. I. Feutrill, P. G. Griffiths, *Aust. J. Chem.* **34**, 2401 (1981); J. Krupa, H. Lessmann, H. Lackner, *Liebigs Ann. Chem.* **7**, 699, (1989).
23. This molecule is not similar to any known precursors of the tetracenomycin C pathway, as described by S. Yue, H. Motamedi, E. Wendt-Pienkowski, and C. R. Hutchinson [*J. Bacteriol.* **167**, 581 (1986)].
24. It is hypothesized that the ketoreduction occurs after the biosynthesis of the complete polyketide chain; see (*7*).
25. R. G. Summers, E. Wendt-Pienkowski, H. Motamedi, C. R. Hutchinson, *J. Bacteriol.* **174**, 1810 (1992).
26. T. A. Voelker *et al.*, *Science* **257**, 72 (1992).
27. H. Fu and C. Khosla, unpublished results.
28. F. Malpartida *et al.*, *Nature* **325**, 818 (1987).
29. G. Muth, B. Nussbaumer, W. Wohlleben, A. Pühler, *Mol. Gen. Genet.* **219**, 341 (1989).
30. D. J. Lydiate, F. Malpartida, D. A. Hopwood, *Gene* **35**, 223 (1985).

31. We thank M. J. Bibb, F. Malpartida, and D. H. Sherman for providing clones and sequence information. We also thank J. E. Bailey, M. J. Bibb, J. I. Brauman, M. Buttner, K. F. Chater, and T. Kieser for valuable comments on the manuscript. Supported in part by grants from the National Science Foundation (BCS-9209901), the American Chemical Society (ACS-PRF 25243-G4), the American Cancer Society (IRG-32-34) to C.K., and by the Camille and Henry Dreyfus New Investigator Award to C.K. D.A.H. acknowledges financial support from the Agricultural and Food Research Council and the John Innes Foundation.

15 July 1993; accepted 12 October 1993

A Binary Source Model for Extension-Related Magmatism in the Great Basin, Western North America

William P. Leeman* and Dennis L. Harry

Models for extension-related magmatism based on decompression melting of asthenospheric mantle poorly simulate fluxes and bulk compositions of magmas produced during early stages of continental extension. For the Great Basin of western North America, it is proposed that magmatism proceeded in two stages, the first involving melting of lithospheric mantle sources between 40 and ~5 million years ago (Ma), followed (since ~5 Ma) by melting of upwelling asthenospheric mantle in areas where extension has exceeded about 100 percent. This transition in magma sources is diachronous, depending on initial variations in lithosphere thickness and on rates of lithospheric thinning.

Magmatism associated with lithospheric extension has been attributed to partial melting of ascending hot mantle material. Such a mechanism reasonably accounts for many aspects of magma production in regions of high extensional strain such as mid-ocean ridge spreading centers and some rifted continental margins (*1*–*3*). However, simple decompression melting is not easily reconciled with styles of magmatism characteristic of early stages of continental rifting. First, unless the lithosphere is unusually thin or an anomalous heat source is present, a significant lag time is predicted between the onset of extension and incipient magmatism because asthenospheric magma sources (for example, "dry" peridotite) must ascend to within ≤~80 km before significant melting occurs (*1*). Second, magma production rates should generally increase with time unless the rate of lithospheric thinning decreases. Third, magma compositions should reflect a progression from deep to progressively shallower depths of melt extraction. These patterns are not always observed. For example, the principal phase of Great Basin extension began at around 40 Ma, after the late Eocene global plate reorganization, and was accompanied by voluminous synextensional silicic magmatism (*4*).

The present Great Basin was the locus of an Andean style magmatic belt until latest Cretaceous or early Paleocene time (~60 to 70 Ma) (*5*). Between ~60 to 40 Ma, magmatism in this region waned and became predominantly alkalic to shoshonitic in character. Local extension began in a belt of now-exhumed metamorphic core complexes along the eastern margin of the Great Basin (*6*). The amount of subsequent extension across this region varies from at

Keith-Wiess Geological Laboratory, Rice University, Houston, TX 77251.

*To whom correspondence should be addressed.